

Semicrystalline Polyimides Based on Controlled Molecular Weight Phthalimide End-Capped 1,3-Bis(4-aminophenoxy)benzene and 3,3',4,4'-Biphenyltetracarboxylic Dianhydride: Synthesis, Crystallization, Melting, and Thermal Stability

Srivatsan Srinivas,[†] Franklin E. Caputo,[‡] Marvin Graham,[§] Slade Gardner,[†] Richey M. Davis,[†] James E. McGrath,[§] and Garth L. Wilkes^{*,†}

Department of Chemical Engineering and Department of Chemistry and NSF Science and Technology Center for High Performance Polymeric Adhesives and Composites, Virginia Tech, Blacksburg, Virginia 24061, and Department of Chemical Engineering, Princeton University, Princeton, New Jersey 08544

Received March 25, 1996; Revised Manuscript Received October 14, 1996[®]

ABSTRACT: The synthesis of controlled molecular weight semicrystalline polyimides based on 1,3-bis(4-aminophenoxy)benzene (TPER diamine) and 3,3',4,4'-biphenyltetracarboxylic dianhydride (BPDA), end capped with phthalic anhydride, is reported herein. The above polyimide henceforth referred to as TPER polyimide ($M_n = 20k, 30k$) displayed excellent thermal stability, as evidenced by dynamic thermogravimetric analysis in both air and nitrogen atmospheres. This polyimide displayed a glass transition temperature of ca. 210 °C based on DSC measurements, and a melting temperature of 395 °C. A unique feature of this polyimide was the fact that quenching the polymer from the melt, even at very high cooling rates (ca. 200 °C/min), did not result in an amorphous polymer, implying very high crystallization rates from the melt. The subsequent melting endotherm was also shown to be extremely narrow, as evidenced by a sharp endotherm in the DSC trace, which was attributed to a narrow distribution of crystal thicknesses. On the basis of the results of the melting behavior of nonisothermally and isothermally crystallized samples, a process of melting/recrystallization has been shown to occur in the system during the DSC heating scan. This melting/recrystallization phenomenon has been shown to give rise to the observed multiple melting endotherms in the DSC scans of isothermally crystallized samples. The equilibrium melting temperature of this polymer estimated using a Hoffman–Weeks plot was shown to be 408 °C. The thermal stability of the TPER-based system has been investigated by monitoring the crystallization and melting response after residence in the melt at various times and temperatures. Melt time and temperature studies showed the exceptional thermal stability of the TPER polyimide versus corresponding results for the commercial polyimide “New TPI” and for a polyimide based on 1,4-bis(4-aminophenoxy)benzene and 4,4'-oxydiphthalic anhydride (TPEQ polyimide). Polyimide samples with amine end groups, as well as samples partially end capped with phthalic anhydride were shown to display distinctly lower thermal stability compared to phthalimide end-grouped samples. The improved behavior was demonstrated by melt rheological and crystallization experiments.

Introduction

Aromatic polyimides are high-performance polymeric materials possessing an exceptional array of properties. Thermal stability, chemical resistance, and excellent mechanical properties have enabled this class of polymer to be used in a variety of applications such as electronic packaging, films, adhesives, and matrix materials for composites.^{1–3} Semicrystalline polyimides offer the further advantages of increased solvent resistance and retention of mechanical properties above the glass transition temperature. These features have made semicrystalline polyimides the focus of considerable research over the recent years.^{4–14}

The rigidity of aromatic polyimides arises from the stiff backbone structure, leading to glass transition and melting temperatures ranging from 200 to above 400 °C. This has led to difficulties in melt processing of polyimides, since 400 °C is nearing the upper bound of

stability for most polymers. Traditional processing has therefore often involved the solution casting of the poly(amic acid) precursor into the desired shape, followed by thermal imidization into the polyimide. However, since melt processing is more desirable from both a cost and environmental safety point of view, the synthesis of melt processable, thermally stable resins is of prime interest. The rigid nature of the chain could also result in the “sluggish” crystallization kinetics of reasonable molecular weight polyimides.

The above stated problems due to high transition temperatures have led to the modification of the backbone structure of polyimides so as to increase flexibility, and thereby lower the transition temperatures. These have included the addition of flexible ether and carbonyl linkages,^{10,11} ethylene glycol sequences,^{13,14} and the incorporation of meta-substituted diamines. Increasing the chain flexibility could also result in an increase in the rate of crystallization; however, lower transition temperatures reduce the effective upper use temperatures of these materials. The goal of our research has therefore focused on the development of thermally stable, fast crystallizing, high-melting polyimides.

Traditional analysis of the thermal stability of polymers has involved the use of thermogravimetric analysis

* To whom correspondence should be addressed.

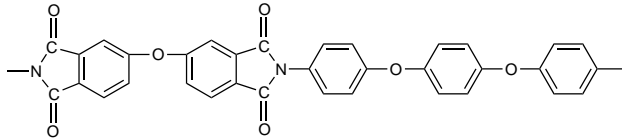
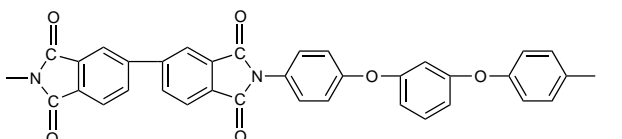
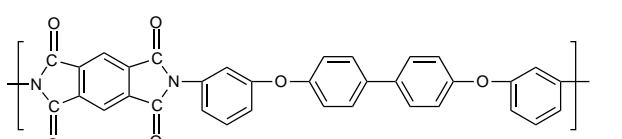
[†] Department of Chemical Engineering, Virginia Tech.

[§] Department of Chemistry and NSF Science and Technology Center, Virginia Tech.

[‡] Department of Chemical Engineering, Princeton.

[®] Abstract published in *Advance ACS Abstracts*, January 15, 1997.

Table 1

	T_g (°C)	T_m (°C)
	238	420
	ca. 210	395
	250	388

(TGA) to evaluate the degradation occurring via weight loss as a function of temperature and/or time. However, degradation reactions such as cross-linking or chain extension could occur with little accompanying weight loss.^{6,15} Therefore, the TGA technique by itself is inadequate for reflecting the thermal stability of the material. Both chain scission as well as cross-linking affect the crystallizability of the polymer; therefore, a more appropriate method than TGA, but indirect measure of thermal stability is the actual crystallization/melting behavior of the material.

This study reports the synthesis and characterization of a high-temperature polyimide based on 1,3-bis(4-aminophenoxy)benzene (TPER diamine) and biphenyl dianhydride (BPDA), end capped with phthalic anhydride. Since the completion of this study we have become aware of recent studies that included the same polyimide studied here.^{16,17} The first section reports the synthesis of the precursor poly(amic acid) and its conversion to the semicrystalline polyimide. The crystallization and melting behavior have been investigated using DSC. The thermal stability has been investigated by monitoring crystallization and melting parameters after exposure to various melt conditions and compared with that of a commercial polyimide, Mitsui Toatsu's Aurum New TPI,^{18–23} and a phthalimide end-capped 1,4-bis(4-aminophenoxy)benzene (TPEQ diamine) and 4,4'-oxydiphthalic anhydride (ODPA) based polyimide,⁶ the structures of which are shown in Table 1. The important effect of end group chemistry on the thermal stability as judged not only by TGA but also via crystallizability and rheological behavior has also been investigated.

Experimental Section

Materials. 1,3-Bis(4-aminophenoxy)benzene (trivially termed triphenyl ether resorcinol diamine, referred to as TPER) was supplied by Ken-Seika Corp. The biphenyl dianhydride (BPDA) was obtained from Chriskev Corp. and dried at 120 °C prior to use. Phthalic anhydride (PA) was obtained from Aldrich and sublimed prior to use. *N*-Methylpyrrolidone (NMP) and 1,2-dichlorobenzene (DCB) were obtained from Fisher and vacuum distilled after drying over P₂O₅ before use.

The commercial polyimide used in this study for purposes of comparison was Mitsui Toatsu's Aurum New TPI, which was available in the form of amorphous extruded film.

The phthalimide end-capped TPEQ/ODPA polyimide used in this study was available in film form, the synthesis and properties of which are referred to in our earlier work.⁶

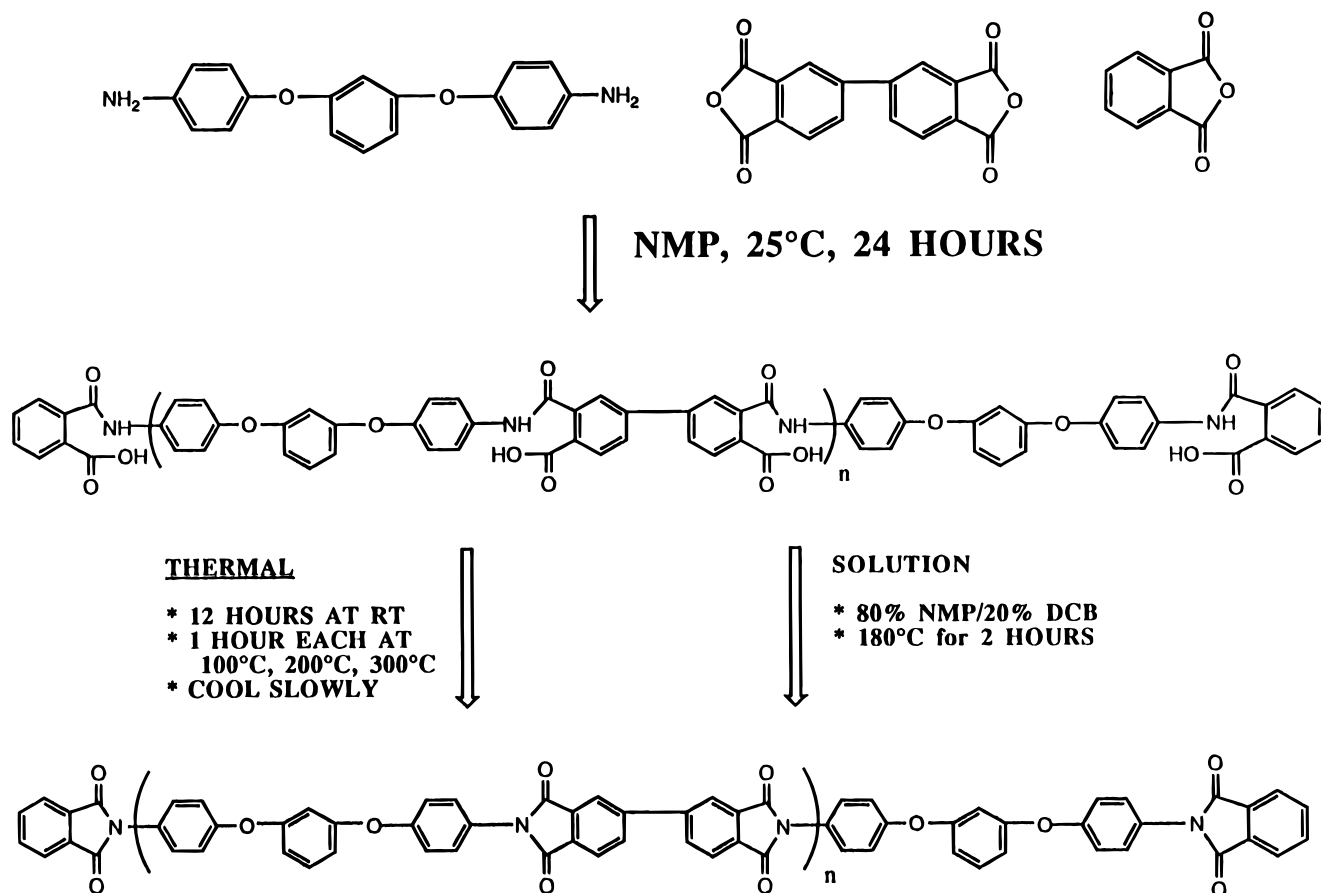
Polymer Synthesis. Polyimides capped with nonreactive phthalimide end groups were synthesized with calculated number average molecular weights of 20 000 and 30 000. A three-neck round bottom flask equipped with a mechanical stirrer, nitrogen inlet and a drying tube, was used as the reaction vessel. The appropriate monomer concentrations for the syntheses were calculated using the Carothers equation. Thus, to the reaction vessel was added a calculated amount of TPER diamine, which was then dissolved in dry NMP. A calculated amount of phthalic anhydride (PA) was then added to the solution. Upon dissolution of the PA, a calculated amount of the dianhydride, BPDA, was added. Enough NMP was added to achieve a 10% solids concentration. This solution was stirred and allowed to react under a nitrogen atmosphere for 24 h, to afford the phthalamic acid end-capped poly(amic acid) as shown in Scheme 1.

The above process was repeated at differing degrees of end capping. A 30 000 M_n amine-terminated poly(amic acid) was synthesized by eliminating all PA from the above described procedure. In addition, a 30 000 M_n "half" (statistical) phthalamic acid end-capped poly(amic acid) was synthesized in which half of the calculated amount of PA needed for full end capping was added to the reaction vessel. For all the polymers described above, the poly(amic acid) solutions were precipitated in cold water to yield solid poly(amic acid). The samples were vacuum dried at 50 °C prior to imidization. An SEC fitted with a viscosity detector was primarily utilized to determine molecular weights of the poly(amic acids) by the procedure described by Konas et al.^{24,25} It was not possible to directly measure the molecular weights of the semicrystalline polyimides since they were insoluble in all suitable solvents. However, independent experience with amorphous systems⁸ has produced nearly identical values before and after imidization.

The poly(amic acid)s were converted to the respective polyimides using two different methods as shown in Scheme 1. In the case of thermal imidization, films of the poly(amic acid) were solvent cast onto glass plates and placed in a drybox in the presence of a nitrogen flow until smooth nontacky films were obtained. The plates were then placed in a vacuum oven, and the temperature raised to 100 °C and held for 1 h. The temperature was then raised to 200 °C, held for 1 h, and finally raised to 300 °C and held for 1 h. The oven was allowed to cool to below 200 °C before removing the films. This imidization procedure, developed by researchers at NASA Langley,²⁶ has been applied by others as well.^{5,6,10–12}

Solution imidization techniques⁸ were also used to obtain the polyimide from the poly(amic acid). In this case, the drying tube used in the apparatus above was replaced with a reverse Dean Stark trap. Dichlorobenzene (DCB) was added as an azeotroping liquid to the solution so as to achieve an 80/20 ratio of NMP to DCB. The solution was heated to about 175 °C and allowed to stir. After about 2 h, partially imidized (ca.

Scheme 1



70%) yellow particulates precipitated from the solution, after which the resulting slurry was poured into water with stirring. The resulting powder was filtered, washed with water, and dried in a vacuum oven overnight at 250 °C and at 300 °C for 1 h to ensure complete imidization. Use of DCB did not cause any technical problems. For the remainder of this paper, the phthalimide end-capped polymer will be referred to as PA end capped, the half phthalimide end-capped polymer as half end capped, and the polymer synthesized with no phthalic anhydride as amine-terminated polyimide. The terminology half end capped is only statistical and does not imply that all molecules are selectively half end capped; rather there is expected to be a distribution of molecules with complete end capping, no end capping (amine functionality) and with half end capping.

Characterization. Thermogravimetric (TGA) studies were carried out on a Seiko TG/DTA on the film samples at heating rates of 10 °C/min under either a nitrogen or air atmosphere. The temperature calibration of the TG/DTA was based on the melting temperatures of indium and zinc. Values reported in this paper are temperatures for 2% weight loss.

The DSC measurements were conducted on a Perkin-Elmer DSC-7, on 6–7 mg of sample under a nitrogen purge, at heating rates of 10 °C/min unless otherwise specified. Temperature and heat flow were calibrated using indium and zinc standards. The DSC curves shown in this paper have been normalized to 1 mg sample mass.

The melt time/temperature studies were carried out on a Seiko DSC 220C using 6–7 mg of sample under a nitrogen purge. The temperature and heat flow were calibrated using indium, tin, and zinc standards. The heating and cooling schedules used in this study were as follows. The samples were heated at 20 °C/min to the various melt temperatures and held for different times. The samples were then cooled at 10 °C/min to room temperature, following which they were reheated at a rate of 10 °C/min. Three parameters were chosen which were representative of the crystallization and melting behavior. The area under the crystallization exotherm

during the cooling scan was denoted as the heat of crystallization. The peak of the melting endotherm during the second heat was taken as the melting temperature, and the area under the endotherm was denoted as the heat of melting. The heating and cooling schedules utilized for the melt time/temperature experiments for New TPI and the TPEQ/ODPA polyimide are described along with the results.

Rheological experiments were carried out on a Bohlin VOR rheometer with a 25 mm diameter parallel plate fixture. A Bohlin HTC using nitrogen as the heating gas was used for temperature control. Both powder as well as film samples of the polyimides ca. 1 mm thick were used in the experiments. The samples were placed between the plates in the HTC oven which was preheated to the required temperature. Approximately 2 min elapsed from the time the sample was placed in the rheometer to when the oven temperature equilibrated to the required temperature, after which the measurements were started. Dynamic oscillatory viscosity data were collected at a frequency of 0.1 Hz and a strain of 2%. The fluids head was used for all measurements along with a 12.54 g cm resistance torque bar.

Results and Discussion

Molecular weights were derived from poly(amic acid) solutions following earlier procedures from our laboratory.^{24,25} A typical raw chromatogram is provided in Figure 1. Actual derived molecular weight values are shown for three samples in Table 2 and are in satisfactory agreement with the targeted values.

The results of the thermogravimetric analyses (TGA) experiments carried out on all samples in air and nitrogen atmospheres are shown in Table 3. By this test, all the samples exhibited excellent thermal stability in air as well as nitrogen, as evidenced by the very high temperatures for 2% weight loss. As expected, the weight loss temperatures were slightly lower in air as

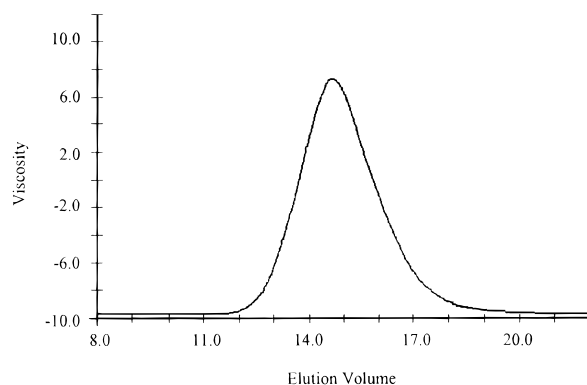


Figure 1. Elution peak of a poly(amic acid) precursor by quantitative size exclusion chromatography.

Table 2. Molecular Weights of Poly(amic acid) Precursors by Quantitative Size Exclusion Chromatography

sample	M_n (calcd)	M_n (exptl)	M_w	M_w/M_n
phthalamic acid (PA) end capped	30 000	27 900	65 800	2.4
half end capped	30 000	27 100	68 300	2.5
amine terminated	30 000	30 900	78 100	2.5

Table 3. Temperatures (°C) for 2% Weight Loss at a Heating Rate of 10 °C/min in Air and Nitrogen

polymer	mol wt	air	nitrogen
TPER-PA	20k	502	539
TPER-PA	30k	526	545
TPER amine terminated	30k	527	549
TPER half end capped	30k	527	549
Aurum New TPI		545	545

compared to nitrogen (ca. 25 °C), except for the case of New TPI. The TGA data suggest that New TPI exhibits superior thermal stability compared to the TPER system. This point will, however, be discussed further with respect to crystallization/melting studies as a function of melt time and temperature. The amine-terminated and half-end-capped polyimide samples showed about the same values for 2% weight loss as the PA end-capped polyimide, thereby implying that the nature of the end group does not influence the thermal stability of the polymer. However, as is also discussed later, the PA end-capped TPER polyimide exhibits superior thermal crystallization stability compared to its partially end-capped and amine-terminated analogues, thus emphasizing a major inadequacy of the TGA technique to provide an accurate indication of structural changes that do not involve weight loss.

DSC Studies. Figure 2 shows the first heat DSC scans for the as-made TPER samples and the New TPI film. All the TPER polymers exhibited weak specific heat jumps corresponding to the glass transition temperature at ca. 230 °C. All the samples exhibited weak endotherms at ca. 295 °C (30k) or 300 °C (20k). Recall that the final step in the thermal imidization cycle involved residence at 300 °C for 1 h. The weak endotherm can therefore be attributed to the melting of less perfect crystals formed at the final imidization temperature. This is followed by broad, weak exotherms corresponding to what is believed to be the result of recrystallization/perfection following the melting of the less perfect crystals. Regardless of the nature of the end group or molecular weight, prominent melting endotherms were observed at ca. 390 °C. The New TPI sample exhibited a prominent glass transition temperature at 250 °C, followed by a cold crystallization

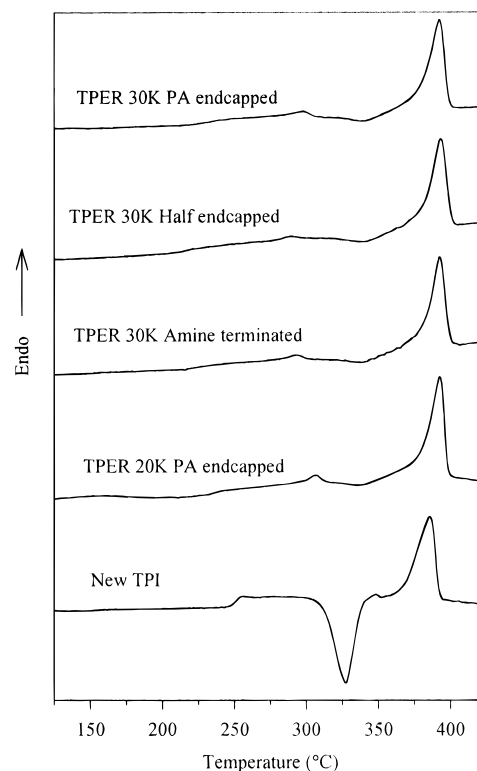


Figure 2. First heat DSC scans for TPER polyimide and New TPI.

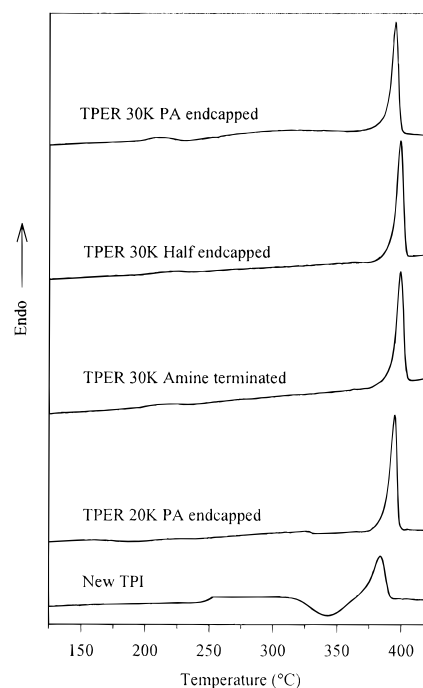


Figure 3. Second heat DSC scans for TPER polyimide and New TPI.

exotherm at 327 °C, and finally a melting endotherm at 385 °C. The samples were held in the melt for 1 min at the end of the first heat (425 °C), rapidly quenched (ca. 200 °C/min) to room temperature, and then reheated.

Figure 3 shows the second heat DSC scans of all the samples. *It is interesting to note that none of the TPER samples could be quenched into a pure amorphous state after the first heat, implying very fast crystallization kinetics of this system.* It is also worth emphasizing that relatively high molecular weight samples were utilized

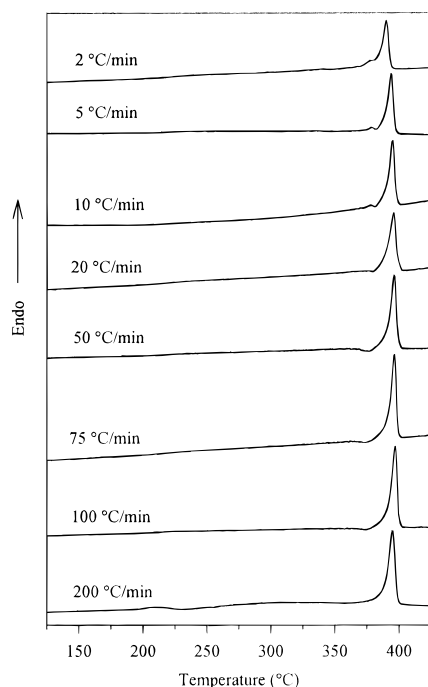


Figure 4. DSC scans for PA end-capped TPER 30k subjected to various cooling rates from the melt.

in this study (20k and 30k). A similar observation was made on a sample of $M_n = 11\,500$ by Hsiao et al.¹⁶ As mentioned in a previous study,⁶ we were able to quench even a 10k TPEQ/ODPA based polymer into a purely amorphous state with relative ease; similar observations have also been made with other polyimide studies in our laboratory.^{4,5} All the TPER samples exhibited weak specific heat transitions corresponding to the glass transition temperature at ca. 210 °C, followed immediately by very weak crystallization exotherms, and finally by sharp melting endotherms at ca. 395 °C. These values of the T_g and T_m are very similar to the earlier reported values^{16,17} on the same system. The unique features of this system include both the extremely fast crystallization kinetics as well as the sharp melting behavior, implying a narrow distribution of crystal thicknesses and perfection. An interesting observation here was that the melting temperatures of the quenched samples of the TPER system were ca. 5 deg greater than that of the as-made samples. Possible causes of this interesting behavior are discussed in the next section. The New TPI sample displayed a glass transition temperature at 250 °C and a somewhat broad crystallization exotherm at 343 °C, followed by a broad melting endotherm at 385 °C; the ease with which this polymer could be quenched into an amorphous state is consistent with earlier reports indicating the extremely slow crystallization kinetics of this polymer.^{18–23}

Melting Studies. The effect of different cooling rates on the subsequent melting behavior of the PA end-capped TPER 30k polyimide was investigated after treatment at 425 °C for 1 min. Figure 4 shows the DSC heating scans at 10 °C/min following various cooling rates from the melt. Clearly, up to a cooling rate of 100 °C/min, the polymer could not be prevented from crystallizing during cooling, as is evident from the lack of a clear glass transition and absence of a crystallization exotherm in the heating scan. At a cooling rate of 200 °C/min, a larger fraction of the polymer could be quenched into the amorphous state, as evidenced by a weak glass transition and crystallization exotherm

during the heating scan. Surprisingly, the melting temperatures as well as the heats of melting were found to increase by 7 deg and by ca. 25%, with increasing cooling rates (except for the case of the sample cooled at 200 °C/min, which displayed a melting temperature slightly lower than that of the sample cooled at 100 °C/min). The peak of the crystallization exotherm during the cooling scan was depressed from 338 °C at 2 °C/min to 300 °C at 100 °C/min. The differences in undercooling would be expected to yield different melting temperatures, with the slower cooling rates displaying slightly higher melting temperatures. At slower cooling rates, the system would experience greater residence times in the crystallization window and hence be expected to yield higher heats of melting as well.

Due to the fast crystallization kinetics, we can reasonably assume that under slow cooling rates, crystallization would occur at low undercoolings under quasi-isothermal conditions and therefore would yield a narrower distribution of more “perfect” and thicker crystals, and a correspondingly lower fraction of “imperfect” and thinner crystals. In contrast, at higher cooling rates, we would expect a much wider distribution of crystal thicknesses and perfection, leading to a wide distribution of melting temperatures. The fraction of crystals that melt at lower temperatures would also be larger compared to the case of the slow-cooled sample.

We hypothesize that these thinner and “imperfect” crystals undergo a process of almost continuous melting and recrystallization/perfection during the DSC heating scan to yield the observed melting endotherm. If the process of melting and recrystallization/perfection is almost simultaneous, we would not necessarily expect any exothermic or endothermic deviations from the baseline. The observations presented here imply that lower melting “imperfect” crystals are more prone to a process of melting and recrystallization/perfection than thicker and more “perfect” crystals. The dependence of the melting temperature and heat of melting on cooling rate can therefore be attributed to melting accompanied by recrystallization/perfection during the DSC heating scan. Further treatment of the recrystallization phenomenon is discussed next. It can also be seen that slower cooling rates result in a dual endothermic behavior, as evidenced by a shoulder on the main melting endotherm, implying that crystallization at lower undercoolings might result in dual melting behavior. This is supported by the following isothermal crystallization studies.

Figure 5 shows the melting endotherms of the PA end-capped TPER 30k samples isothermally crystallized at various temperatures after a melt treatment at 420 °C for 5 min. Multiple endotherms are quite evident in the melting behavior for samples crystallized in the range 325–370 °C. These results are similar to those reported earlier by Hsiao et al.^{16,17} except that our results encompass a wider range of crystallization temperatures. For crystallization temperatures (T_c) between 325 and 370 °C, the lowest endotherm (peak I) is observed at temperatures of ca. $T_c + 10$ °C. An intermediate endotherm (peak II) is observed at crystallization temperatures from 330 to 370 °C, which first appears as a low temperature shoulder on the main melting endotherm (peak III) and gradually increases in size and temperature with increasing crystallization temperature. The high-temperature endotherm (peak III) is initially independent of crystallization temperature (until a T_c of 340 °C) after which it shows a slight

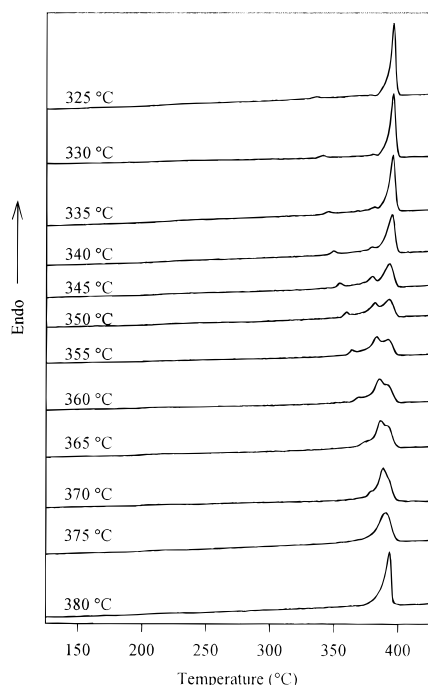


Figure 5. DSC scans for PA end-capped TPER 30k samples isothermally crystallized at various temperatures.

decrease and then remains essentially independent of crystallization temperature. The size of peak III decreases in size relative to the size of peak II with increasing crystallization temperature, until it appears as a shoulder on the high-temperature side of peak II. At crystallization temperatures of 375 °C and higher, only a single endotherm is observed.

The origin of the multiple endothermic behavior has already been explained by Hsiao et al. in their previous work^{16,17} on the basis of X-ray diffraction and heating rate experiments. We will present some further evidence to support their explanations. In previous studies^{16,17} as well as our studies, samples were cooled to room temperature at the end of the crystallization step before subsequent heating in the DSC. In order to investigate if the cooling run at the end of the crystallization gave rise to any of the endotherms, a sample was heated at the end of the crystallization step without first cooling to room temperature. The positions and sizes of the melting endotherms were, in this case, essentially identical to the case when the samples were first cooled to room temperature, implying that cooling to room temperature prior to the heating scan did not give rise to any of the endotherms. The multiple endotherms are therefore characteristic of the isothermal crystallization, and/or the subsequent heating scan. The effect of crystallization time on the melting endotherms was investigated by crystallizing samples for different times at 345 °C, at which temperature the primary crystallization process was complete within 5 min. As shown in Figure 6, the position and relative sizes of the upper two endotherms were independent of crystallization time. However, the position as well as the size of the lowest endotherm (peak I) increased linearly with the log of annealing time. The dependence of peak I on crystallization temperature and time as shown in Figures 5 and 6 is consistent with the trends reported for the annealing ($T_c + 10$) endotherm for other polymers.^{19,27} Though there has been considerable debate in the literature^{27–35} on the origin and nature of the $T_c + 10$ °C endotherm, evidence favors the

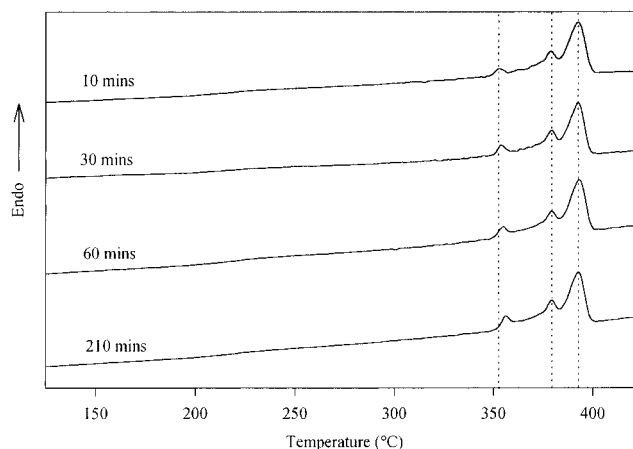


Figure 6. DSC scans for PA end-capped TPER 30k isothermally crystallized at 345 °C for various times.

explanation that this endotherm arises as a result of the melting of thinner lamellae that are formed as a result of secondary crystallization at the crystallization/annealing temperature. These thinner lamellae are believed to be formed as separate stacks in the amorphous regions between primary lamellar stacks. Thus, at this stage we can confirm the origin of the lowest endotherm (peak I) as due to the melting of thin “in-filling” lamellae that are formed as a result of secondary crystallization at the crystallization temperature, an explanation that was also put forward previously.^{16,17}

Our heating rate and X-ray diffraction experiments gave essentially the same results as those reported by Hsiao et al.,^{16,17} which confirmed that polymorphism was not the origin of the multiple melting behavior, rather that peak II was indicative of the dominant crystals formed at the isothermal crystallization temperature, and melting/recrystallization of these crystals during the DSC scan gave rise to peak III. Since the upper endotherm (peak III) is formed as a result of the reorganization process, its position would be expected to be independent of the crystallization temperature, which in fact is observed in our study. However, since peak II is representative of the melting of pre-existing crystals, its temperature would be expected to increase with crystallization temperature, which in fact is again observed here.

On the basis of the assignment of peak II to the primary crystals formed at the isothermal crystallization temperature, we have constructed a Hoffman–Weeks plot to estimate the equilibrium melting temperature of this polymer. This value is typically obtained using extrapolative techniques such as the Gibbs–Thomson method³⁶ or the Hoffman–Weeks method.³⁶ The more common method is the Hoffman–Weeks method which requires the melting temperatures (T_m) of samples crystallized at different temperatures (T_c) to be plotted against each other, and the line joining them to be extrapolated to the $T_m = T_c$ line, the point of intersection being the equilibrium melting temperature T_m° . The peak temperatures of the three endotherms have been plotted as a function of crystallization temperature in Figure 7. The points corresponding to peak I are parallel to the $T_m = T_c$ line, thereby ruling out peak I as arising from primary crystals formed at the isothermal crystallization temperature (though it should be noted that the position of peak I is also a function of crystallization time). The peak III values are almost independent of crystallization temperature, and in fact show a small decrease at $T_c = 345$ °C, after

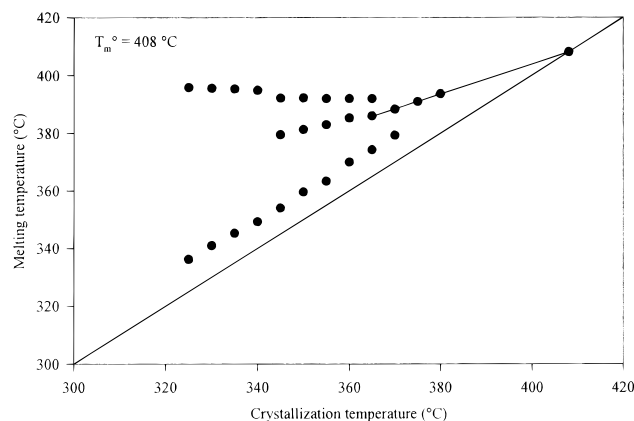


Figure 7. Hoffman–Weeks plot for PA end-capped TPER 30k polyimide.

which it is again independent of crystallization temperature. This again reinforces the earlier statement that the endotherm corresponding to peak III does not represent the melting of crystals formed at the isothermal crystallization temperature. The values corresponding to peak II temperatures were therefore utilized in order to make the extrapolation. The value of the equilibrium melting temperature determined this way was found to be 408 °C, a value very similar to that reported earlier of 410 °C.¹⁶ Two points regarding this method should be emphasized: first that the values of the melting temperatures were determined by using the peak of the second endotherm from the DSC scan. Due to the overlapping melting/recrystallization events, the observed DSC thermogram is a convolution of simultaneously occurring melting endotherms and a recrystallization exotherm. The real value of the peak of the melting endotherm is therefore likely somewhat different from that observed in the DSC. This introduces some uncertainty in the values of the melting temperatures determined from a DSC trace. The second point to be emphasized here is that since the Hoffman–Weeks procedure is an extrapolative procedure, any errors/uncertainties in evaluating either T_c or T_m could lead to large variations in the value of T_m^0 determined from the plot. Hence the value of the equilibrium melting temperature determined from this plot should be treated at best as a semi-quantitative estimate of the real value.

The melting/recrystallization process has been shown to occur for all cases of melt-crystallized samples. A point worth noting here is that the as-made sample exhibited a broad melting endotherm, implying a broad distribution of crystal thicknesses and perfection. This sample did not seem to undergo a process of melting/recrystallization during the DSC heating scan. Recall also that the as-made sample had undergone a complex crystallization history consisting of a stepwise thermal imidization cycle, during which the poly(amic acid) was converted to the crystallizable polyimide, accompanied by loss of solvent and water. Since the crystallization history of the as-made sample is quite complex, we will not attempt to speculate as to why this sample did not undergo a process of melting/recrystallization during the initial DSC scan.

Thermal Stability. The thermal stability of the PA end-capped TPER 30k polymer was compared to the stability of New TPI and the earlier studied PA end-capped TPEQ/ODPA system.⁶ The effect of the nature of the end group was also investigated by comparing the thermal stability of the PA end-capped TPER 30k system with that of the amine-terminated and half-end-

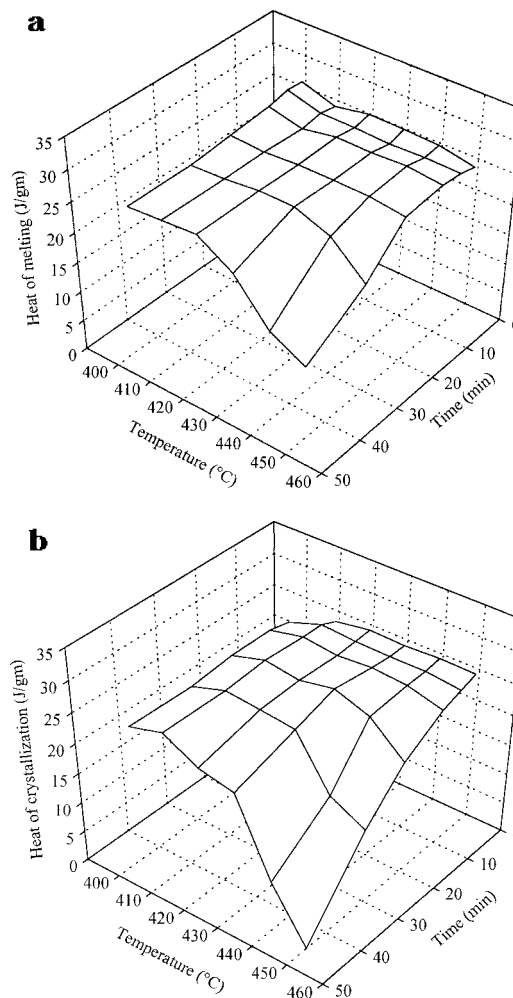


Figure 8. (a) Effect of time and temperature in the melt on the heat of melting of PA end-capped TPER 30k. (b) Effect of time and temperature in the melt on the heat of crystallization of PA end-capped TPER 30k.

capped TPER 30k polymers. As discussed earlier, the parameters characterizing the crystallization and melting processes were plotted as a function of melt time and melt temperature in order to gain information on the melt thermal stability of these polyimides.

The area under the melting endotherm (heat of melting) for the PA end-capped TPER 30k polymer is shown in Figure 8a as a function of time and temperature in the melt. *Each grid point on the 3D plot represents a specific thermal history.* This 3D plot assists in the qualitative understanding of the effect of thermal history on the melting behavior, as it relates to changes in nucleation density and/or chemical changes in the polymer. The exceptional thermal stability of this polymer is evident from the figure. It is obvious that melt times up to 45 min at temperatures as high as 420 °C did not depress the heat of melting. A melt temperature of 420 °C is not only ca. 25 deg above the observed melting temperature but also could be above the equilibrium melting temperature, as suggested from the Hoffman–Weeks analysis discussed earlier. At a melt temperature of 430 °C, there was no change in the heat of melting up to a time in the melt of 30 min. Even at temperatures as high as 450 °C, the heat of melting remained unchanged for times as high as 20 min! *Thus, this study shows that any processing operation of this material can involve temperatures of 420–430 °C, for times up to 30 min, and still maintain the original heat of melting characteristics.* At a time of 45 min, for

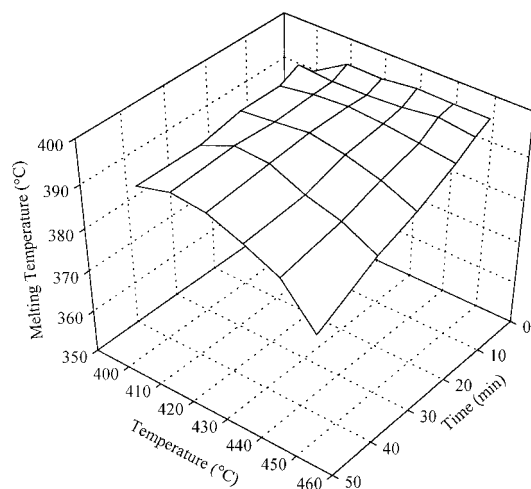


Figure 9. Effect of time and temperature in the melt on the melting temperature of PA end-capped TPER 30k.

temperatures above 420 °C, or at a temperature of 450 °C for times above 20 min, there was, however, a drop in the heat of melting, implying a reduction in the degree of crystallinity. This is presumably caused by chemical changes in the material induced by chain branching/cross-linking, as evidenced by an increase in the melt state viscosity, the results of which are discussed later.

The heat of crystallization (area under crystallization exotherm) dependence on the time and temperature in the melt is shown in Figure 8b. The dependence of the heat of crystallization on melt conditions is qualitatively the same as the heat of melting shown in Figure 8a, except that the drop in the heat of crystallization occurs under less harsh melt conditions than the heat of melting. For example, under melt conditions of 420 °C and 45 min, the heat of melting did not show any drop; however, the heat of crystallization was lower as compared to the value at a melt condition of 410 °C, 45 min. Under the most harsh condition studied here, i.e. 450 °C, 45 min, there was no crystallization exotherm on cooling; however, the heat of melting showed a value that was about 50% of that observed under less harsh conditions. This is because some crystallization occurred during the heating scan in the DSC, as was evidenced by an exotherm observed immediately above the glass transition, which gave rise to a melting endotherm during the subsequent heating scan. Except for the case of harsh melt conditions, the heat of melting was essentially the same as the heat of crystallization. *This has important implications for the processing of this material, since the above data indicate that a substantial fraction of crystallinity is developed during the cooling scan, and a post-processing annealing step might well be unnecessary in order to generate crystallinity.*

Changes in melting temperatures versus exposure times at varying melt temperatures are shown in Figure 9. An interesting point to note here is the fact that there is actually an increase in the melting temperature when the melt residence temperature increases from 400 to 410 °C. Recall that 400 °C is just at the tail end of the melting endotherm and below the equilibrium melting temperature. The melting temperature decreased with increasing melt temperatures for the case of the higher melt times, i.e. 20, 30, and 45 min, this decrease being prominent only at the highest melt time of 45 min. The maximum decrease in the melting temperature was observed to be ca. 14 deg on changing the melt time from

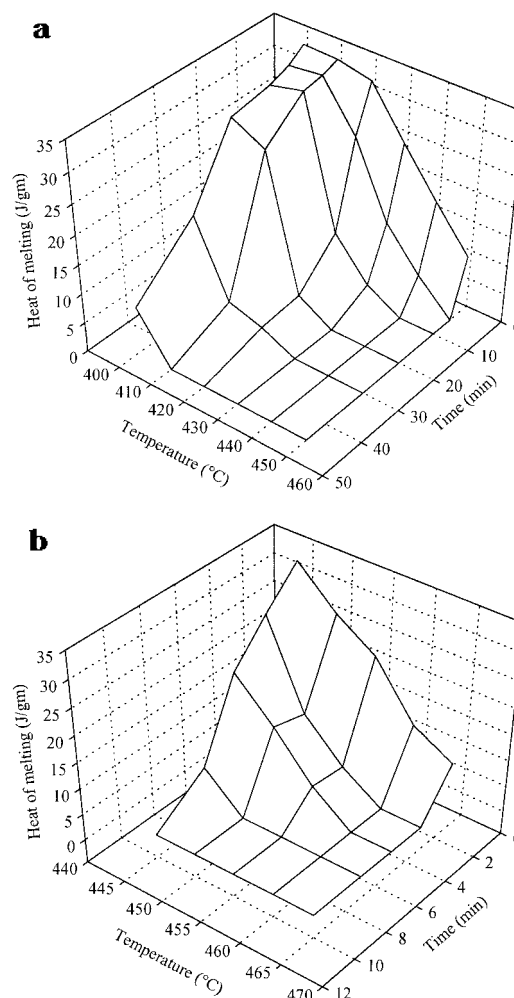


Figure 10. (a) Effect of time and temperature in the melt on the heat of melting of New TPI. (b) Effect of time and temperature in the melt on the heat of melting of PA end-capped TPEQ/ODPA polyimide.

1 to 45 min at a melt temperature of 450 °C. Under potentially reasonable processing conditions (420 °C, 30 min) the melting temperature did not exhibit any decrease, implying that under these conditions there was no substantial change in the chemical structure of the polymer. This, combined with the earlier findings regarding the heat of crystallization and heat of melting, presents strong evidence in favor of the exceptional thermal stability of this polymer. The fact that the melting temperature and the heat of melting did not change under the same conditions that the heat of crystallization decreased (Figure 8b) indicates that this decrease was likely due to changes in nucleation density. The decrease in melt temperature with harsher melt conditions is likely due to the fact that chemical changes like chain branching/cross-linking occur, leading to the formation of imperfect crystals.

The variation of heat of melting of Aurum New TPI as a function of melt time and temperature is shown in Figure 10a. Since the crystallization kinetics of New TPI were very slow on cooling from the melt, samples of New TPI were quenched from the melt, and reheated at 10 °C/min. This caused crystallization to occur from the glass during the DSC heating scan. In contrast to the behavior exhibited by the TPER 30k polymer, the heat of melting of New TPI showed a strong dependence on the prior thermal history, in that higher temperatures and longer times in the melt caused the heat of melting to exhibit sharp decreases. The decrease in the

heat of melting was more prominent at higher melt temperatures and longer melt times. For example, at a melt temperature of 420 °C, the heat of melting decreased to one-eighth of its original value when the melt time was increased from 1 to 30 min; this was accompanied by a 4 deg decrease in melting temperature as well. This decrease in the heat of melting of the New TPI polyimide with increasing time/temperature in the melt arises as a result of changes in both nucleation density as well as chemical changes like chain branching/cross-linking occurring in the melt.

Figure 10b shows the variation of the heat of melting of a PA end-capped TPEQ/ODPA polyimide as a function of time and temperature in the melt. Due to the slow crystallization kinetics of this system, samples of this polymer were also quenched from the melt and reheated in order to study the crystallization and melting behavior. As for the case of New TPI, this polyimide also showed a strong dependence on the melt conditions, in that higher melt temperatures and longer melt times hindered the ability of the material to recrystallize. The decrease in the heat of melting was accompanied by a decrease in the melting temperature, again implying that chemical changes occurred in the melt leading to an increase in molecular weight.⁶

The above figures clearly emphasize the fact that the PA end-capped TPER 30k material shows superior thermal stability with respect to the crystallizability and melting characteristics. A simple TGA study revealed only that the 2% weight loss temperatures indicated excellent thermal stability and were misleading, in that the results indicated that New TPI displayed superior thermal stability compared to the TPER system.

The effect of varying end group chemistry on the thermal stability of the material was also investigated, keeping in mind that the TGA studies indicated only that the 2% weight loss temperatures were independent of the nature of the end group. The DSC heating and cooling schedules used in this study were as follows: the samples were heated at 20 °C/min to 430 °C, held for 30 min, following which they were cooled at a rate of 10 °C/min to room temperature. The samples were then heated at 10 °C/min up to 425 °C. Figure 11a shows the DSC cooling scans of the three samples; the PA end-capped sample exhibited a prominent crystallization exotherm, consistent with the data presented earlier regarding the excellent thermal stability of this material. The half-end-capped sample exhibited only a small crystallization exotherm, indicating the reduced ability of this material to crystallize during the cooling scan. The amine-terminated sample did not exhibit any exotherm during the cooling scan, implying that the melt treatment had suppressed the ability of this material to crystallize. Figure 11b shows the subsequent DSC heating scans; the PA end-capped sample displayed a weak glass transition, no exothermic activity beyond the glass transition region, and a melting endotherm. The half-end-capped sample displayed a glass transition, followed by a crystallization exotherm and a melting endotherm. The melting temperature of the half-end-capped sample was lower than that of the PA end-capped sample. The amine-terminated sample displayed a prominent glass transition, showed no evidence of any prominent exothermic event, and finally showed a weak melting endotherm, the position of which was lower compared to the other two samples. The data indicate the pronounced effect the end group nature has on the crystallization response after a melt treatment.

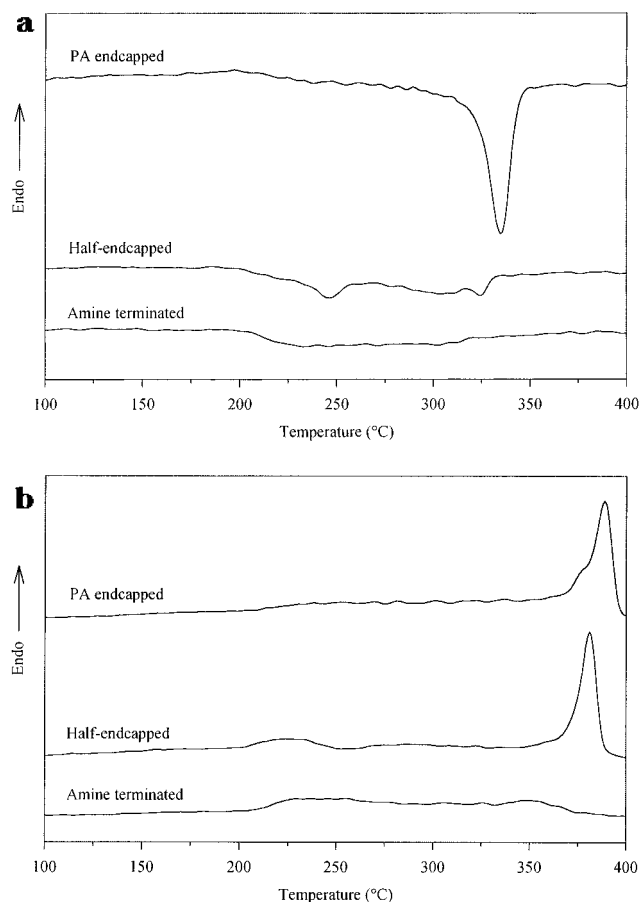


Figure 11. (a) DSC cooling scans for TPER 30k polyimide samples with different end groups after a melt history of 430 °C, 30 min. (b) DSC heating scans for TPER 30k polyimide samples with different end groups after cooling as shown in Figure 11a.

It is clear that the PA end-capped samples were not affected by a melt treatment of 430 °C for 30 min. The half-end-capped sample was clearly affected by the melt treatment in that the ability of the material to crystallize during the cooling scan was suppressed, due to an increase in molecular weight as evidenced by a rapid increase in melt viscosity as is discussed in the next section. During the subsequent reheat, however, the polymer could crystallize due to the increased nucleation density, resulting in a melting endotherm observed in the DSC scan. The depression of the melting temperature compared to the PA end-capped polymer possibly results from the more imperfect crystals formed due to the chemical changes, such as transimidization in the material. The melt treatment resulted in the almost complete suppression of the crystallizability of the amine-terminated sample, again due to an increase in polymer molecular weight, to a greater extent than for the half-end-capped sample, as shown by a greater increase in the melt viscosity. This increase in molecular weight prevented the polyimide from crystallizing not only during the cooling scan but also during the subsequent reheat as well. The few crystals that were formed were very imperfect which resulted in a minor endotherm observed at relatively low temperatures. The end group study shows that effective end capping of polyimides by phthalic anhydride (PA) groups greatly improves the thermal stability of the polymer. Amine end groups are most susceptible to chain branching/cross-linking reactions leading to an increase in molecular weight and lower crystallizability. The half-end-

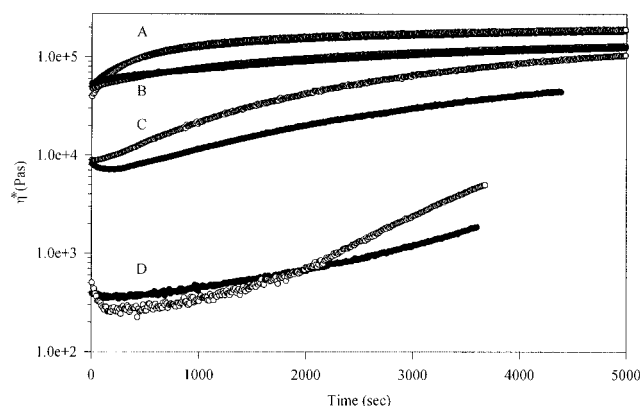


Figure 12. Isothermal viscosity sweeps for PA end-capped TPER samples and New TPI at different temperatures. Curves A: TPER 30k powder, (○) 430 °C, (●) 420 °C. Curves B: TPER 30k film, (○) 430 °C, (●) 420 °C. Curves C: TPER 20k film, (○) 420 °C, (●) 418 °C. Curves D: New TPI film, (○) 430 °C, (●) 420 °C.

capped polymer displays behavior that is intermediate to that of the PA end-capped polymer and the amine-terminated system.

Rheological Studies. Thermal stability of the polyimides under harsh melt conditions was probed with rheological techniques since melt viscosity is critically dependent on the molecular weight of the system. Isothermal viscosity sweeps were carried out on PA end-capped TPER 20k film, TPER 30k film, and TPER 30k powder (imidized in solution as discussed earlier), as well as New TPI film, as is shown in Figure 12. Curves A represent the viscosity of the TPER 30k powder sample, with the open circles denoting the isothermal behavior at 430 °C, and the solid circles the response at 420 °C. Curves B represent the viscosity dependence for the TPER 30k film, with the open circles representing the behavior at 430 °C, and the solid circles the behavior at 420 °C. Curves C are the viscosity dependence of the TPER 20k film (open circles, 426 °C; solid circles, 418 °C). Curves D are the viscosity response of New TPI (open circles, 430 °C; solid circles, 420 °C).

For all the samples studied here, the viscosity increased with time, implying an increase in molecular weight. This is speculated to occur due to chain branching/cross-linking reactions in the melt. At present we cannot offer an explanation for the viscosity differences between the TPER 30k powder and the TPER 30k film, but the imidization conditions used to prepare these samples could have resulted in differences in end group chemistry. For the case of the TPER powder samples, the viscosity increased by a factor of almost 3 after 30 min at 420 °C; for the case of the TPER film samples, the viscosity increased only by ca. 65% under similar conditions.

For the TPER 30k samples, there seems to be no appreciable difference in the change in viscosity with time on the log scale displayed in the figure for samples held at 420 and 430 °C. However, when plotted on a smaller scale, it was obvious that the viscosity increase was more prominent at 430 °C compared to 420 °C, implying that residence at higher melt temperatures caused an increase in the rate of the chemical changes giving rise to the branching/cross-linking reactions, as would be expected. The early time viscosity was, however, lower at a melt temperature of 430 °C as compared to 420 °C.

For the case of the TPER 20k sample at 418 °C, the viscosity increased by a factor of 2 after 30 min in the

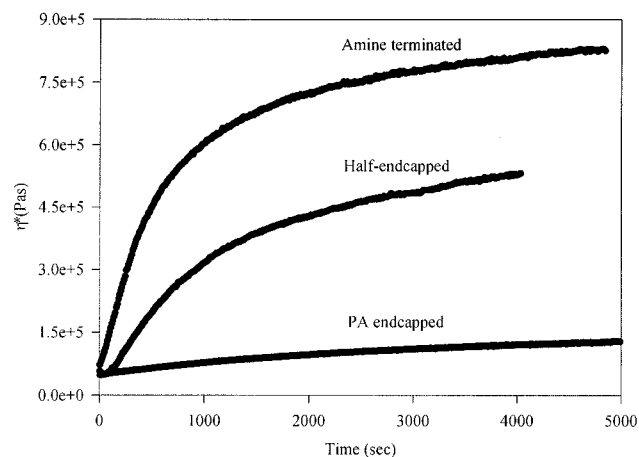


Figure 13. Isothermal viscosity sweeps for TPER 30k polyimide with different end groups at 430 °C.

melt; at a melt temperature of 426 °C, the viscosity increased to almost 4 times the original value over the same time period. The rate of increase in viscosity as a function of melt time was greater for the 20k polymer as compared to the 30k system, especially at higher temperatures. This could perhaps be attributed to the presence of a larger fraction of end groups in the lower molecular weight system, which could imply that any chemical changes occurring in the melt could involve the end groups.

For the case of New TPI, the viscosity did not show any appreciable increase for times up to 30 min at melt temperatures of 420 and 430 °C, implying no appreciable molecular weight changes occurred in the system. Recall that in this same time range, the DSC results indicated a major decrease in the crystallizability of the New TPI system. This decrease in crystallizability cannot thus be attributed to any appreciable changes in molecular weight. The drop in crystallizability can thus be at least partially attributed to changes in nucleation density of the polymer due to the melt treatment. The decrease in the melting temperature of the New TPI polyimide with increasing melt time and temperature, however, indicates some chemical changes occurring in the system. These chemical changes could occur without any substantial increase in molecular weight and is possibly the major cause of the drastic reduction in crystallizability of this polymer with increasing melt time/temperature.

The TPER polymer used in this study was a relatively high molecular weight polymer, available in the form of creasable films. Mechanical properties studies (not shown here) carried out at room temperature indicated that the semicrystalline films of the TPER system exhibited considerable toughness, as evidenced by the high strain to break. The New TPI material was, however, of lower molecular weight, as evidenced not only by the lower melt viscosities but also by the fact that once crystallized, the films were extremely brittle, i.e. showed very low strain to break and poor creasability. In spite of this difference in molecular weight, the TPER polyimide showed very fast rates of bulk crystallization, whereas the New TPI system could easily be quenched into an amorphous form.

The isothermal viscosities for samples with different end groups as a function of time in the melt at 430 °C are shown in Figure 13. The rate of increase in viscosity increased in the order amine end capped > half end capped > PA end capped, clearly emphasizing, therefore, the importance of end groups in determining the

high-temperature stability of polyimides. Amine end groups seem to be much more susceptible to chain extension/branching/cross-linking than phthalimide end groups which is consistent with basic considerations. The viscosity increase explains the decrease in crystallizability of the amine-terminated and half-end-capped polyimides as compared to the completely end-capped system after residence in the melt and is consistent with the results reported in the previous section.

Conclusions

The synthesis and characterization of a 20k and 30k M_n all aromatic polyimide displaying high transition temperatures (T_g and T_m) have been reported here. This polyimide is based on phthalimide end-capped 1,3-bis-(4-aminophenoxy)benzene (TPER diamine) and 3,3',4,4'-biphenyltetracarboxylic dianhydride (BPDA). Excellent thermal stability of this system is concluded from TGA studies, melt time and temperature studies on the DSC, and rheological studies. Rheological as well as crystallization studies showed that the nature of the end groups played a critical role in determining the thermal stability of these polyimides. Polyimide samples with no nonreactive end capping (amine end groups) and half end capped with phthalic anhydride exhibited distinctly lower thermal stability in the melt compared to a PA end-capped system, as evidenced by large viscosity increases causing a dramatic decrease in the crystallizability. In spite of the reasonably high molecular weight and high melt viscosity of this polymer, this system displayed extremely fast crystallization kinetics, evidenced by the inability to quench this polymer into the fully amorphous state. The lower molecular weight New TPI material displayed a lower melt viscosity but showed much slower crystallization kinetics, as evidenced by the ease with which this material could be quenched into the amorphous state. The apparent lower molecular weight of the New TPI studied here also resulted in a very brittle, low toughness behavior of the crystallized sample, which was in contrast to the TPER films which showed nonbrittle behavior resulting in very good creasability. Even though the TGA results indicated the superior thermal stability of New TPI as compared to the TPER polyimide, a more detailed DSC investigation of melt time/temperature effects showed the superior stability characteristics of the TPER polyimide with respect to the crystallization and melting behavior.

The melting behavior of this polymer showed some unique features which included the sharp melting endotherm after nonisothermal as well as isothermal crystallization. The melting endotherm of the as-made sample was, however, observed to be broad. This behavior of the melting endotherms has been attributed to a broad distribution of crystal thicknesses for the as-made sample, and a narrow distribution of crystal thicknesses for a slow-cooled sample. The melting behavior of this polymer included multiple melting endotherms (peaks I–III) which have been assigned to a $T_c + 10^\circ\text{C}$ type endotherm (peak I), the melting of the crystals present in the sample before the DSC scan (peak II), their subsequent recrystallization followed by melting to yield the highest temperature endotherm (peak III). Imperfect crystals and thin crystals have been shown to be more susceptible to melting/recrystallization than thicker and more perfect crystals.

Acknowledgment. The authors would like to acknowledge the NSF Science and Technology Center for

High Performance Polymeric Adhesives and Composites for full support of this study under contract number DMR 9120004. F.E.C. would also like to thank the NSF Center for support under the Summer Undergraduate Research Program at Virginia Tech.

References and Notes

- (1) Feger, C. J.; Khojasteh, M. M.; McGrath, J. E., Eds. *Polyimides: Materials, Chemistry and Characterization*; Elsevier Science Publishers B.V.: Amsterdam, 1989.
- (2) Mittal, K. L., Ed., *Polyimides: Synthesis, Characterization and Applications*; Plenum: New York, 1984; Vols. 1 & 2.
- (3) Wilson, D.; Stenzenberger, H. D.; Hergenrother, P. M., Eds. *Polyimides*; Blackie & Son Ltd.: Glasgow and London, 1990.
- (4) Muellerleile, J. T.; Risch, B. G.; Rodrigues, D. E.; Wilkes, G. L.; Jones, D. M. *Polymer* **1992**, *34*, 789.
- (5) Brandom, D. K.; Wilkes, G. L. *Polymer* **1995**, *36*, 4083.
- (6) Srinivas, S.; Graham, M.; Brink, M. H.; Gardner, S.; Davis, R. M.; McGrath, J. E.; Wilkes, G. L. *Polym. Eng. Sci.* **1996**, *36*, 1928.
- (7) Rogers, M. E.; Brink, M. H.; Brennan, A.; McGrath, J. E. *Polymer* **1993**, *34*, 849.
- (8) Kim, Y. J.; Glass, T. E.; Lyle, G. D.; McGrath, J. E. *Macromolecules* **1993**, *26*, 1344.
- (9) Brink, M. H.; Brandom, D. K.; Wilkes, G. L.; McGrath, J. E. *Polymer* **1994**, *35*, 5018.
- (10) Hergenrother, P. M.; Wakelyn, N. T.; Havens, S. J. *J. Polym. Sci., Polym. Chem. Ed.* **1987**, *25*, 1093.
- (11) Hergenrother, P. M.; Havens, S. J. *J. Polym. Sci., Polym. Chem. Ed.* **1989**, *27*, 1161.
- (12) Hergenrother, P. M.; Beltz, M. W.; Havens, S. J. *J. Polym. Sci., Part A: Polym. Chem.* **1991**, *29*, 1483.
- (13) Heberer, D. P.; Cheng, S. Z. D.; Barley, J. S.; Lien, H. S.; Bryant, R. G.; Harris, F. W. *Macromolecules* **1991**, *24*, 1890.
- (14) Cheng, S. Z. D.; Heberer, D. P.; Lien, H. S.; Harris, F. W. *J. Polym. Sci., Part B: Polym. Phys.* **1990**, *28*, 655.
- (15) Cella, J. A. *Polym. Degrad. Stab.* **1992**, *36*, 99.
- (16) Kreuz, J. A.; Hsiao, B. S.; Renner, C. A.; Goff, D. L. *Macromolecules* **1995**, *28*, 6926.
- (17) Hsiao, B. S.; Kreuz, J. A.; Cheng, S. Z. D. *Macromolecules* **1996**, *29*, 135.
- (18) Friler, J. B.; Cebe, P. *Polym. Eng. Sci.* **1993**, *33*, 587.
- (19) Huo, P. P.; Cebe, P. *Polymer* **1993**, *34*, 696.
- (20) Huo, P. P.; Friler, J. B.; Cebe, P. *Polymer* **1993**, *34*, 4387.
- (21) Brillhart, M. V.; Cebe, P. *J. Polym. Sci., Part B: Polym. Phys.* **1995**, *33*, 927.
- (22) Lu, S. X.; Cebe, P.; Capel, M. *J. Appl. Polym. Sci.* **1995**, *57*, 1359.
- (23) Hsiao, B. S.; Sauer, B. B.; Biswas, A. *J. Polym. Sci., Part B: Polym. Phys.* **1994**, *32*, 737.
- (24) Konas, M.; Moy, T. M.; Rogers, M. E.; Shultz, A. R.; Ward, T. C.; McGrath, J. E. *J. Polym. Sci., Part B: Polym. Phys.* **1995**, *33*, 1429.
- (25) Konas, M.; Moy, T. M.; Rogers, M. E.; Shultz, A. R.; Ward, T. C.; McGrath, J. E. *J. Polym. Sci., Part B: Polym. Phys.* **1995**, *33*, 1441.
- (26) Bell, V. L.; Stump, B. L.; Gager, H. *J. Polym. Sci.* **1976**, *14*, 2275.
- (27) Hsiao, B. S.; Sauer, B. B.; Verma, R. K.; Zachmann, H. G.; Seifert, S.; Chu, B.; Harney, P. *Macromolecules* **1995**, *28*, 6931.
- (28) Blundell, D. J.; Osborn, B. N. *Polymer* **1983**, *24*, 953.
- (29) Lee, Y.; Porter, R. S. *Macromolecules* **1987**, *20*, 1336.
- (30) Lee, Y.; Porter, R. S.; Lin, J. S. *Macromolecules* **1989**, *22*, 1756.
- (31) Bassett, D. C.; Olley, R. H.; Al Raheil, I. A. M. *Polymer* **1988**, *29*, 1745.
- (32) Lattimer, M. P.; Hobbs, J. K.; Hill, M. J.; Barham, P. J. *Polymer* **1992**, *33*, 3971.
- (33) Cebe, P.; Hong, S. *Polymer* **1986**, *27*, 1183.
- (34) Verma, R. K.; Kander, R. G.; Velikov, V.; Marand, H.; Hsiao, B. S.; Chu, B. *Bull. Am. Phys. Soc.* **1994**, *39*, 109.
- (35) Jonas, A. M.; Russell, T. P.; Yoon, D. Y. *Macromolecules* **1995**, *28*, 8491.
- (36) Hoffman, J. D.; Davis, G. T.; Lauritzen, J. L. *Treatise on Solid State Chemistry*; Hannay, N. B., Ed.; Plenum: New York, 1976; Vol. 3.